


RESEARCH ARTICLE

Open Access



MUS81 cleaves TOP1-derived lesions and other DNA–protein cross-links

Victoria Marini^{1,2}, Fedor Nikulenkov¹, Pounami Samadder¹, Sissel Juul³, Birgitta R. Knudsen³ and Lumir Krejci^{1,2,4*} 

Abstract

Background DNA-protein cross-links (DPCs) are one of the most deleterious DNA lesions, originating from various sources, including enzymatic activity. For instance, topoisomerases, which play a fundamental role in DNA metabolic processes such as replication and transcription, can be trapped and remain covalently bound to DNA in the presence of poisons or nearby DNA damage. Given the complexity of individual DPCs, numerous repair pathways have been described. The protein tyrosyl-DNA phosphodiesterase 1 (Tdp1) has been demonstrated to be responsible for removing topoisomerase 1 (Top1). Nevertheless, studies in budding yeast have indicated that alternative pathways involving Mus81, a structure-specific DNA endonuclease, could also remove Top1 and other DPCs.

Results This study shows that MUS81 can efficiently cleave various DNA substrates modified by fluorescein, streptavidin or proteolytically processed topoisomerase. Furthermore, the inability of MUS81 to cleave substrates bearing native TOP1 suggests that TOP1 must be either dislodged or partially degraded prior to MUS81 cleavage. We demonstrated that MUS81 could cleave a model DPC in nuclear extracts and that depletion of TDP1 in MUS81-KO cells induces sensitivity to the TOP1 poison camptothecin (CPT) and affects cell proliferation. This sensitivity is only partially suppressed by TOP1 depletion, indicating that other DPCs might require the MUS81 activity for cell proliferation.

Conclusions Our data indicate that MUS81 and TDP1 play independent roles in the repair of CPT-induced lesions, thus representing new therapeutic targets for cancer cell sensitisation in combination with TOP1 inhibitors.

Keywords DNA-protein cross-links repair, MUS81, TDP1, Topoisomerase 1

Background

DNA-protein cross-links occur when a protein gets covalently bound to DNA. They represent toxic lesions that may interfere with replication and transcription progression [1]. DPCs can be formed by exogenous or endogenous agents and have non-enzymatic or enzymatic origins. Non-enzymatic DPCs occur when a protein is non-specifically cross-linked to the DNA and are frequently induced by chemicals such as cisplatin, endogenous reactive oxygen species or UV light. Enzymatic DPCs result from the activity of enzymes whose covalent reaction intermediates get trapped on DNA due to the presence of a poison or damaged bases in proximity [2–5]. Among these, the topoisomerases trapped on DNA belong to the most studied type of DPCs. Topoisomerases

*Correspondence:

Lumir Krejci
lkrejci@chemi.muni.cz

¹ Department of Biology, Masaryk University, Kamenice 5/B07, Brno 62500, Czech Republic

² International Clinical Research Center, Center for Biomolecular and Cellular Engineering, St. Anne's University Hospital Brno, Pekařská 53, Brno 60200, Czech Republic

³ Department of Molecular Biology and Genetics, Aarhus University, Universitetsbyen 81, Aarhus 8000, Denmark

⁴ National Centre for Biomolecular Research, Masaryk University, Kamenice 5/C04, Brno 625 00, Czech Republic



© The Author(s) 2023. **Open Access** This article is licensed under a Creative Commons Attribution 4.0 International License, which permits use, sharing, adaptation, distribution and reproduction in any medium or format, as long as you give appropriate credit to the original author(s) and the source, provide a link to the Creative Commons licence, and indicate if changes were made. The images or other third party material in this article are included in the article's Creative Commons licence, unless indicated otherwise in a credit line to the material. If material is not included in the article's Creative Commons licence and your intended use is not permitted by statutory regulation or exceeds the permitted use, you will need to obtain permission directly from the copyright holder. To view a copy of this licence, visit <http://creativecommons.org/licenses/by/4.0/>. The Creative Commons Public Domain Dedication waiver (<http://creativecommons.org/publicdomain/zero/1.0/>) applies to the data made available in this article, unless otherwise stated in a credit line to the data.

are essential enzymes in the DNA metabolism that release topological stress arising from the nature of the double-helical structure of DNA [6, 7]. These ubiquitous enzymes cleave DNA and form a transient covalent bond between a tyrosine in the active site and a phosphoryl group at the DNA break site, creating the so-called cleavage complex. This step is followed by the relaxation and religation of DNA with the concomitant liberation of the entire protein [7]. Human topoisomerase I (TOP1) cleaves only one DNA strand, to which it binds at the 3' end [6]. A TOP1 cleavage complex (TOP1cc) may endure when occurring near a single-stranded break, near modified bases that impede DNA religation [8, 9] or in the presence of a TOP1 poison (such as camptothecin, CPT) [10]. Trapped TOP1ccs have been suggested to interfere with the replication or transcription, causing the arrest of the moving replication fork and leading to the formation of a double-strand break (DSB) [11–16]. The collision of the replication fork with TOP1cc triggers a DNA damage response and arrest of the cell cycle in the G2 phase [17]. Given the requirement of topoisomerase activities, Top1ccs, together with other DPCs, represent a serious threat to the cell. Several pathways have evolved to repair these lesions by targeting the DNA, the protein or the linking bond [1–5, 18].

One such pathway involves tyrosyl-DNA phosphodiesterase 1 (Tdp1), a protein that has been identified to be responsible for the removal of Top1ccs through hydrolysis of the 3'-phosphodiester bond [19–21]. Nevertheless, studies in *Saccharomyces cerevisiae* indicate that alternative repair pathways can also remove Top1 lesions since deletion of the *TDP1* gene does not induce higher sensitivity to CPT [22–25]. This was further supported by the observation that *RAD9* deletion sensitises *tdp1Δ* strain to CPT [20, 22]. Similarly, the disruption of *RAD52* in yeast enhances the cytotoxicity of CPT [13, 26, 27], suggesting the generation of DSBs and a role of homologous recombination (HR) in the repair of Top1ccs. Recently, a protease Wss1/SPRTN-dependent repair pathway has also been identified as required for the repair of DPCs [25, 28–31]. Finally, several nucleases, including Mus81-Mms4, Mre11 and Rad1-Rad10, have been linked with the repair of Top1ccs [32–35]. However, their role in DPCs processing is still not well defined.

MUS81 is the catalytic subunit of the heterodimeric complexes MUS81-EME1 and MUS81-EME2 in humans and Mus81-Mms4 in budding yeast (for simplicity, referred to as MUS81-EME1, MUS81-EME2 and Mus81-Mms4, respectively). These proteins belong to the XPF/MUS81 protein family, which plays an important role in DNA repair. All MUS81 complexes possess structure-specific endonuclease activity and preferentially cleave branched DNA substrates, including 3' flap, replication fork and nicked Holliday junction in vitro [36–39]. The

MUS81 protein has been shown to play a role in the resolution of recombinant intermediates and replication fork stability [27, 40–43] and has been implicated in the repair of mitomycin C- or cisplatin-induced cross-links [44, 45].

In this study, we aimed to test the ability of Mus81-Mms4, MUS81-EME1 and MUS81-EME2 complexes to cleave DNA-protein cross-links, particularly those bearing covalently bound TOP1. To this end, we prepared a series of DNA substrates that mimic a DNA-protein lesion as well as substrates covalently linked to TOP1. Our biochemical data suggest that MUS81 can remove TOP1, but similarly to TDP1, it requires the proteolytic degradation of TOP1 within the cleavage complex to achieve this process. Moreover, the simultaneous depletion of MUS81 and TDP1 in cells suggests that MUS81 plays a backup role to TDP1 in the DNA damage response. Importantly, since compounds inducing TOP1-mediated DPCs are currently used in cancer treatment [46–48], understanding the underlying mechanism of the repair pathway is essential for improving the efficiency of combination therapy with TDP1 and MUS81 inhibitors.

Results

Mus81-Mms4 and MUS81-EME1 cleave various fluorescein-modified substrates

To test whether Mus81-Mms4 and MUS81-EME1 can cleave substrates with a DPC lesion, we first created substrates modified only with fluorescein. The fluorescein molecule also serves to mimic the tyrosine group of TOP1 active site [49]. The nuclease activity assay was performed with two substrates, a 3' flap with fluorescein attached at the 3' end of the single-stranded flap and a nicked duplex with fluorescein at the 3' end of the nick (Additional file 1: Fig. S1A). The DNA substrates were incubated with increasing amounts of Mus81-Mms4 or MUS81-EME1, and the reaction mixtures were analysed by native PAGE. As shown in Fig. 1B, C, both Mus81-Mms4 and MUS81-EME1 were fully capable of cleaving these substrates with comparable efficiency to the 3' flap substrate labelled at the bottom strand (Additional file 1: Fig. S1B and Fig. 1A). These data suggest that fluorescein at the 3' end of a flap or nick, mimicking a tyrosine residue, does not represent an obstacle to the nuclease activity of these enzymes.

To verify that the activity we observe with the nicked duplex is specific to MUS81, we compared wild-type (WT) and a nuclease-dead (ND) mutant of MUS81. For this purpose, we used a truncated version of the complex, MUS81(246–551)-EME1(178–570) [50] and ND mutant containing D338A and D339A mutations [51]. To better monitor the cleavage, the nicked duplex was labelled with two fluorescent dyes: fluorescein and CY5

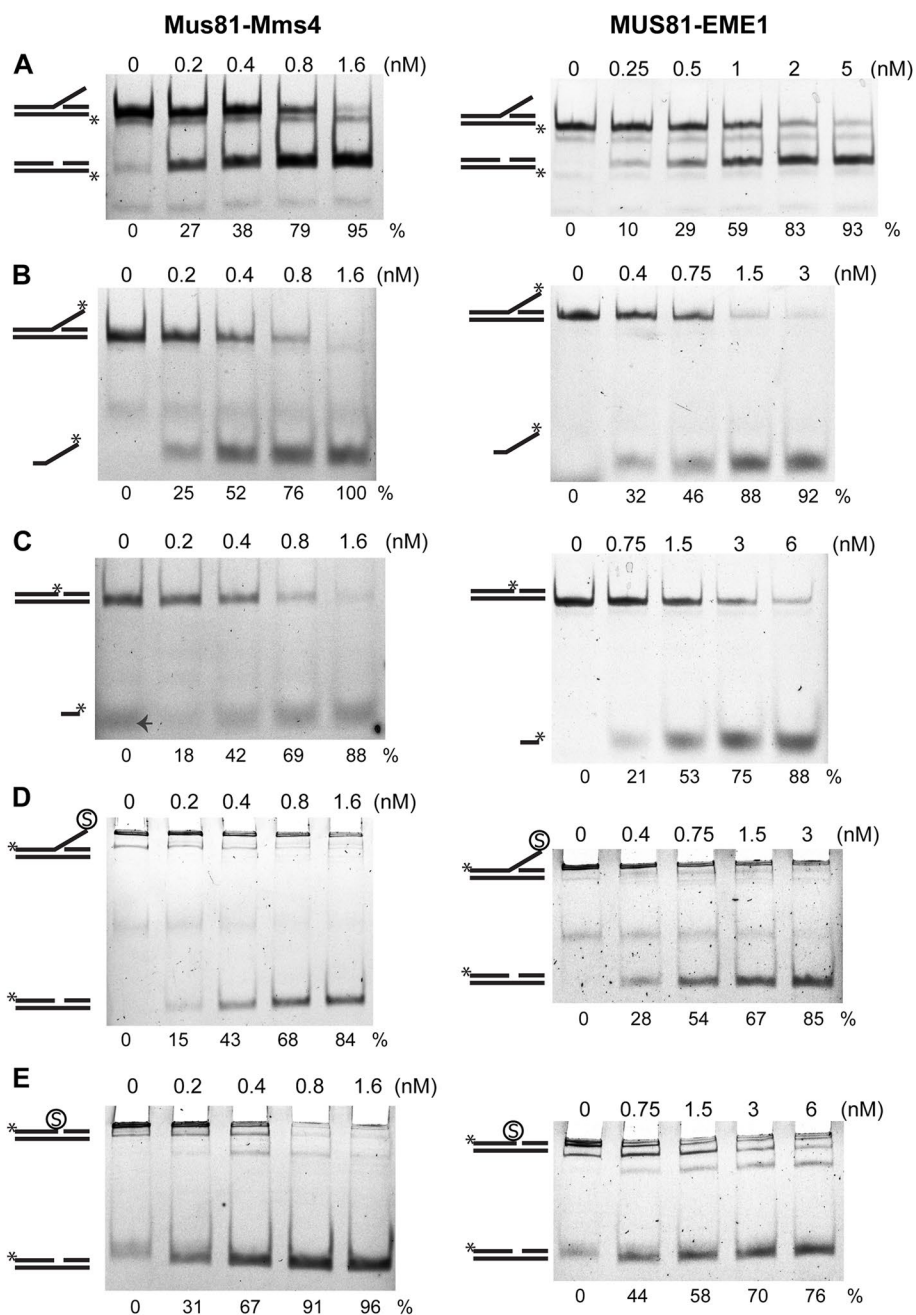


Fig. 1 Mus81-Mms4 and MUS81-EME1 cleave fluorescein and streptavidin substrates. The nuclease activity assay for Mus81-Mms4 and MUS81-EME1 was performed by mixing the DNA substrate with the indicated protein complex concentrations and incubating for 15 min at 30 °C or 37 °C, respectively. The samples were resolved by native PAGE. The asterisk marks the position of fluorescein. Mus81-Mms4 and MUS81-EME1 efficiently cleave standard 3' flap substrate (**A**), nicked duplex and 3' flap substrates containing the fluorescein label at the 3' end of the cleaved strand (**B, C**), and nicked duplex and 3' flap with streptavidin (S) attached to the 3' end of the cleaved strand (**D, E**). Numbers under the gel pictures represent the percentage of cleavage product calculated from the sum of substrate and product band intensities, except for the reaction with the streptavidin substrates, where the substrate band intensity of the control lane was taken as 100%. A small arrow (**C**) indicates Orange G containing the loading buffer used in that particular lane for gel migration control

at the 3' end of the nick and the 5' end of the bottom strand, respectively (Additional file 2: Fig. S2A). While incubation of the WT complex cleaved the substrates in

a concentration-dependent manner, no products were obtained with the ND complex (Additional file 2: Fig. S2A). These data confirm the intrinsic MUS81 nuclease

activity requirement for cleavage of the nicked duplex. Next, we checked the cleavage position of MUS81-EME1 within the nicked duplex, using two substrates with fluorescein either at the 3' end of the nick or at the 5' end of the same oligonucleotide together with CY5 label at the 5' end of the bottom strand (Additional file 2: Fig. S2B). The incubation of the MUS81-EME1 complex with these substrates showed no cleavage of the bottom strand and endonucleolytic processing of the 3' end of the nick. This cleavage is similar to the one observed for Mus81-Mms4 complex [37].

Streptavidin does not prevent cleavage by Mus81-Mms4 or MUS81-EME1

To further analyse the results obtained with the fluorescein modification, we tested the effect of a bulkier modification compared with that of a sole tyrosine residue. Therefore, we designed substrates containing a biotin group to which streptavidin could be attached. Two streptavidin-bound substrates, a 3' flap and a nicked duplex (Additional file 1: Fig. S1C), were incubated with increasing amounts of Mus81-Mms4 or MUS81-EME1. The reaction mixtures were analysed as mentioned above. Both substrates were very efficiently cleaved by both Mus81-Mms4 and MUS81-EME1 (Fig. 1D, E). Although the substrate containing streptavidin remained very close to the gel wells, the cleaved substrate could run further into the gel. Based on this result, we conclude that even a 60-kDa bulky protein does not block the nucleolytic cleavage of the substrate by the tested nuclease complexes.

Native TOP1 prevents cleavage

While streptavidin attached to DNA through the biotin group may not interact with the DNA itself, TOP1 is known to embrace DNA (PDB 1A31 [52]); PDB 1K4S [53]). To test whether this affects the nuclease activity, we used a suicide substrate, with TOP1 covalently bound to a nicked duplex and in the native state as previously described (Additional file 1: Fig. S1D) [54, 55]. The substrate was incubated with increasing amounts of MUS81-EME1 or TDP1, and the samples were loaded on native PAGE. However, we did not observe any cleavage by MUS81-EME1 (Fig. 2A) nor by TDP1 (Fig. 2B), suggesting that native TOP1 makes the cleavage site inaccessible for cleavage by MUS81-EME1 or TDP1.

TDP1 and MUS81 activity requires the proteolytical processing of TOP1-conjugated substrates

It has been proposed that TOP1 must undergo proteolysis to facilitate the removal of the resulting peptide from DNA by TDP1 [56]. Thus, we reasoned that the MUS81 endonucleases would also cope with the trapped TOP1

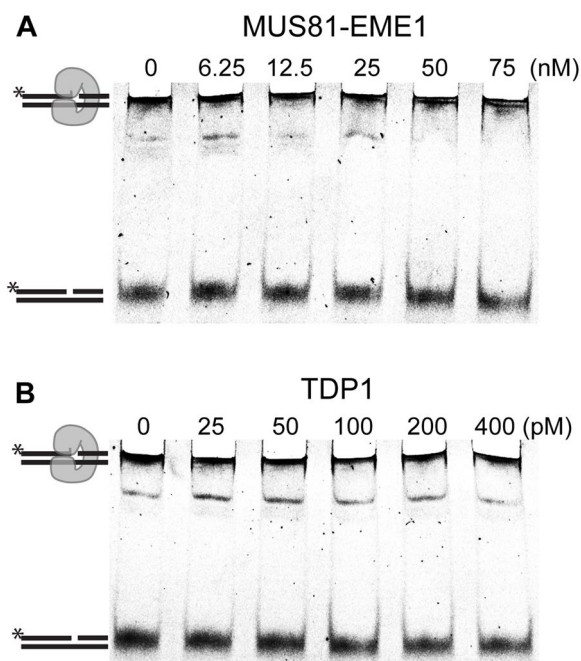


Fig. 2 MUS81-EME1 and TDP1 cannot remove TOP1 in a native state. The substrate bearing native TOP1 covalently bound to the 3' end of the nick was mixed with the indicated amounts of MUS81-EME1 or TDP1, and the mixture was incubated for 15 min at 37 °C for MUS81-EME1 or at 30 °C for TDP1. Neither MUS81-EME1 (A) nor TDP1 (B) can cleave the native TOP1 substrate. The reaction was stopped with SDS in both cases, and the samples were run on native PAGE

after its processing. To address this, we prepared suicide substrates containing the covalently bound TOP1 and treated them with trypsin (“Methods”, Additional file 3: Fig. S3 and Additional file 4: Supplementary Methods). Using this procedure, we designed three substrates, as depicted in Additional file 1: Fig. S1E. The slower-migrating band corresponds to the substrate cleaved by TOP1 and bears the remaining peptide (oligo 7 + TOP1 peptide). The faster band corresponds to the unmodified DNA substrate (oligo 7) due to not fully efficient DNA cleavage by TOP1 (Additional file 3: Fig. S3B and C).

The above-described substrates were incubated with TDP1 or MUS81-EME1 proteins, and the samples were analysed by denaturing PAGE. As expected, TDP1 was able to remove the TOP1 peptide very efficiently from all three modified substrates while leaving the unmodified substrates intact, indicating the specificity of the reaction toward modified DNA (Fig. 3A). MUS81-EME1 is also able to entirely cleave the nicked duplex (Fig. 3B) and the trypsinised 3' flap (Fig. 3C) with similar efficiency as for unmodified substrates (note the disappearance of both the upper and lower bands of the substrate, Additional file 5: Fig. S4A). Because the Y-form substrate is not suitable for

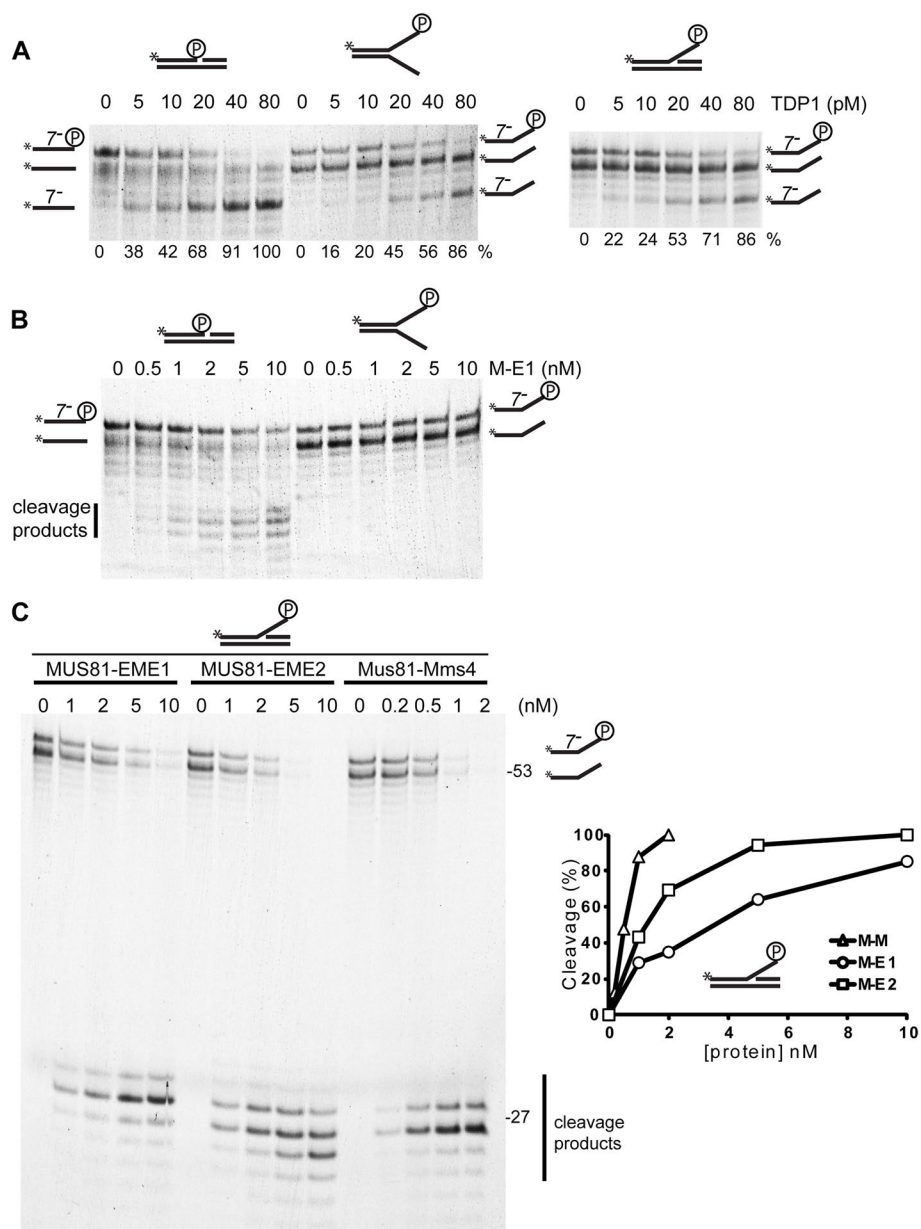


Fig. 3 Trypsinised DNA substrates and their cleavage by TDP1 and MUS81 complexes. DNA substrates bearing a small TOP1 peptide were prepared by treating TOP1-linked DNA with trypsin. **A** TDP1 removes the TOP1 peptide from nicked duplex, Y-form and 3' flap. The trypsinised substrates were incubated with TDP1 at 30 °C for 15 min. The reaction was stopped with SDS and resolved by denaturing PAGE. Numbers under the gel pictures represent the percentage of cleavage product calculated from the sum of the modified substrate and product band intensities. **B** MUS81-EME1 (M-E1) cleaves trypsinised nicked duplex in contrast to Y-form DNA. **C** Mus81-Mms4 (M-M), as well as MUS81-EME1 (M-E1) and MUS81-EME2 (M-E2), efficiently cleave the trypsinised 3' flap substrate (left). Quantification of the activity (right). Only the bands corresponding to the oligo 7⁻ bearing the small TOP1 peptide were quantified. The trypsinised substrates were incubated with increasing amounts of MUS81 complexes at 37 °C for 15 min. The reaction was stopped by adding SDS and resolved by denaturing PAGE

MUS81 endonucleases, we also did not observe any cleavage of the trypsinised Y-form (Fig. 3B).

To assess whether this activity is conserved, we also performed the assays with Mus81-Mms4 and MUS81-EME2. As shown in Fig. 3C, all complexes were able to fully cleave

the trypsinised 3' flap with similar efficiency as the unmodified substrate (Fig. 3C and Additional file 5: Fig. S4). Moreover, we observed that Mus81-Mms4 and MUS81-EME2 were even more efficient nucleases than MUS81-EME1 (Fig. 3C), in accordance with previously published data [39].

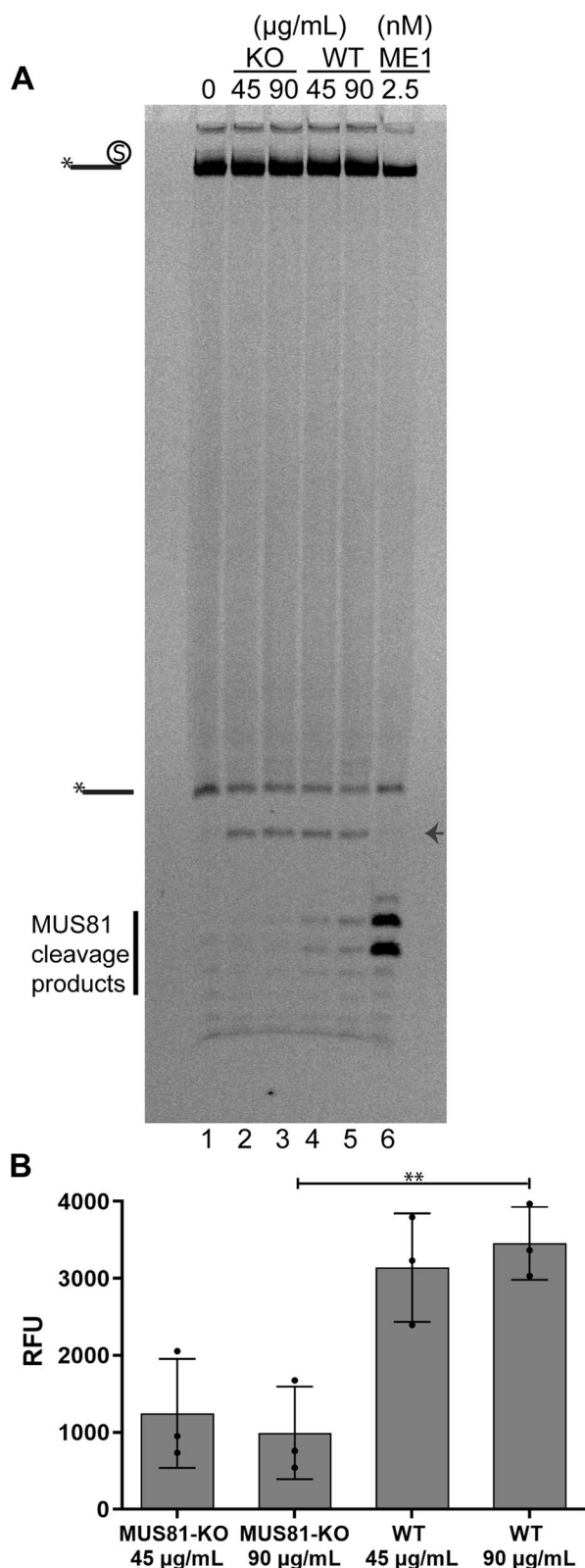


Fig. 4 Cleavage of DPCs by MUS81 in nuclear extracts. **A** A nicked duplex modified with streptavidin was incubated with different amounts of nuclear extracts from CAL51 MUS81-KO (lanes 2 and 3) or WT CAL51 (lanes 4 and 5) cells at 37 °C for 1 h. The reaction was also performed with recombinant MUS81-EME1 complex (2.5 nM, lane 6). The small arrow indicates an unspecific band, most likely the product of the removal of the biotin moiety from the residual oligonucleotide without streptavidin. **B** Quantification of the reaction products from **A**. Relative fluorescence units (RFU) are the arbitrary units of the imaging system for fluorescence intensity. The means and standard deviations from three independent experiments are shown. The *P* value (***P* < 0.01) was calculated through an unpaired two-tailed *t*-test. Individual data values can be found in Additional file 10

MUS81 complex cleaves streptavidin-modified nicked duplex in human nuclear extracts

Our biochemical analysis shows that MUS81 endonucleases may play a role in the repair of TOP1 lesions and other DPCs. To address this role in cells, we tested the processing of DPC-like substrates using nuclear cell extracts. To this end, we generated a MUS81 knockout CAL51 cell line using CRISPR/Cas9 and confirmed the loss of MUS81 protein expression (Additional file 6: Fig. S5A). Next, we prepared nuclear extracts from CAL51 WT and MUS81-KO cell lines and incubated them with a DPC-mimicking substrate, i.e. nicked duplex-bearing streptavidin at the 3' end of the nick (Additional file 1: Fig. S1F). We included phosphorothioate bonds to protect the other free ends of the substrate from exonuclease degradation. We observed distinguishable bands in CAL51 WT extracts that matched cleavage sites of this DPC substrate by recombinant MUS81-EME1 complex (Fig. 4A, lanes 4–6). Accordingly, these bands reduced to background signal in the CAL51 MUS81-KO extract sample (Fig. 4A, lanes 2 and 3 and Fig. 4B), indicating that MUS81 also cleaves such a model DPC in a cell-free setting.

MUS81 represents an alternative pathway to TDP1

To confirm the role of the human MUS81 in processing DPCs and its relationship with TDP1 in cells, we examined the sensitivity of cells to low doses of CPT in the presence or absence of these two proteins. Using specific siRNA, we depleted TDP1 in CAL51 WT and MUS81-KO cells (Fig. 5A) and assessed cell proliferation by the WST-1 assay. While at given conditions, loss of MUS81 or TDP1 alone had no significant effect on the cells' sensitivity, their combination showed CPT concentration-dependent sensitisation (Additional file 6: Fig. S5B), indicating that both TDP1 and MUS81 are involved in the processing of TOP1-mediated DPCs.

Furthermore, we observed that even without CPT treatment, CAL51 MUS81-KO cells and TDP1

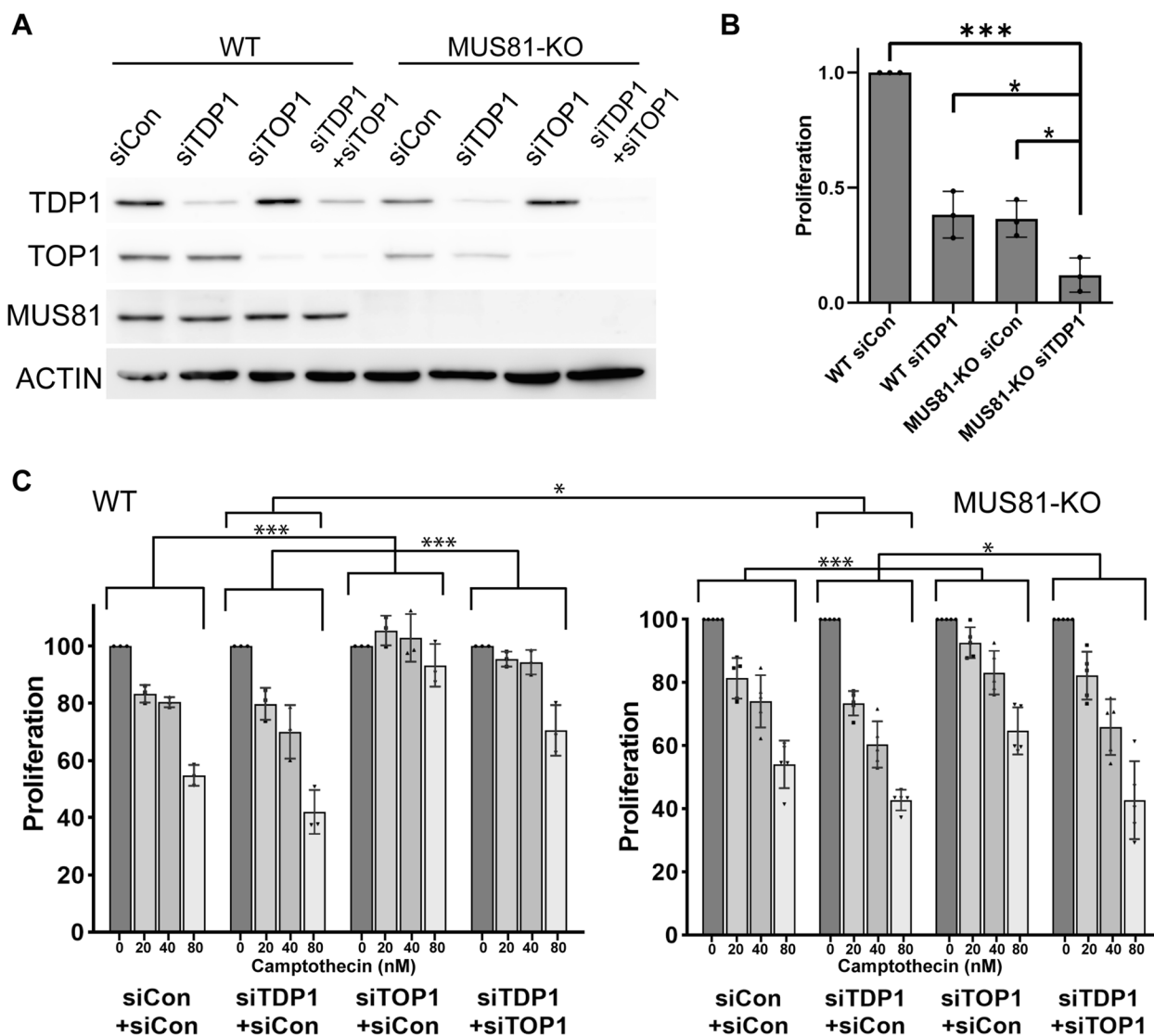


Fig. 5 Depletion of TDP1 sensitises MUS81-KO cells to CPT and affects their proliferation. **A** The efficiency of TDP1 and TOP1 knockdown in CAL51 WT and MUS81-KO cells was determined by Western blot. Actin was used as a loading reference. **B** The proliferation of untreated CAL51 WT and MUS81-KO cells with or without TDP1 depletion was measured by WST-1 assay. The means and standard deviations from three independent experiments are shown. The *P* values were calculated through an unpaired two-tailed *t*-test (**P* < 0.05, ****P* < 0.001). Individual data values can be found in Additional file 10. **C** Cell proliferation of CAL51 WT and MUS81-KO cells simultaneously treated with corresponding siRNA (siCon, siTDP1, or siTOP1) and the presence of increasing CPT concentrations. To maintain the amount of siRNA of the double mutant in all samples, extra siCon was added for single-depleted and control cells. The means and standard deviations from three (WT) and five (KO) independent experiments are shown. The statistical significance was determined by two-way ANOVA test (**P* < 0.05, ****P* < 0.001). Individual data values can be found in Additional file 10

downregulated CAL51 cells showed slower proliferation (Fig. 5B). Interestingly, the depletion of TDP1 in CAL51 MUS81-KO cells led to an additional decrease in cell proliferation, further supporting the role of TDP1 and MUS81 in separate pathways.

When treating CAL51 WT cells with higher CPT concentrations, we observed a reduction in proliferation, which is almost completely reversed after TOP1

depletion (Fig. 5C). Depletion of TDP1 exacerbates the effect of CPT and is also rescued by the simultaneous co-depletion of TOP1, even though to a lesser extent than WT cells. Next, we performed the same experiments in CAL51 MUS81-KO cells and cells co-depleted for TDP1 (Fig. 5C). In contrast to MUS81-KO cells, the proliferation of TDP1/MUS81 double deficient cells was only slightly improved upon depletion of TOP1, indicating a

possible role of MUS81 and TDP1 in the repair of TOP1-independent lesions.

Discussion

Genetic experiments in budding yeast have shown the existence of TOP1cc repair pathways involving various nucleases, including Mre11, Rad1-Rad10 or Mus81-Mms4 [22, 32, 33]. Because Mus81-Mms4 and MUS81-EME1 have been shown to be involved in the repair of stalled replication forks and cleave 3' flap and fork-like substrates *in vitro*, we wished to determine the role of MUS81 in the removal of DPCs.

This study showed that the cleavage of a 3' flap or a nicked duplex by Mus81-Mms4 and MUS81-EME1 is not impaired by the fluorescein positioned at the 3' end of the cleaved strand to imitate a remaining active site tyrosyl moiety of TOP1 attached to DNA. Moreover, streptavidin attached to the 3' end of the cleaved strand also does not prevent MUS81 from cleaving the tested substrates, which contrasts with the substrate containing TOP1 in its native state. Since the structure of TOP1 covalently bound to a short DNA duplex shows the formation of a clamp around DNA with the TOP1-DNA linkage buried inside the protein [52] in contrast to streptavidin that does not bind DNA, our results indicate that the MUS81 nuclease activity is not compromised by the presence of a large protein as long as the cleavage site for MUS81 is accessible. This is further supported by the ability of MUS81 to cleave proteolytically processed TOP1ccs. Similarly, we show that also TDP1 cannot efficiently cleave TOP1 in its native state, in agreement with previously reported data [56–58]. The requirement for the proteolytical processing of DPCs has also been indicated by the fact that the inhibition of the proteasome results in a less-efficient repair of DPCs [59, 60]. CPT-induced DSBs in cells also depend on the proteasomal activity and polyubiquitination of TOP1 [61, 62]. On the other hand, other studies have demonstrated that CPT-dependent DSBs do not depend on proteasomal activity [63, 64]. This might, however, reflect the identification of other proteases involved in processing DPCs. The budding yeast Wss1, a DNA-dependent protease, was shown to play a role in the repair of Top1cc through the proteolysis of Top1 [25]. Cells lacking *WSS1* and *TDP1* present a hypersensitivity to CPT that is suppressed by the disruption of the *TOP1* gene, suggesting that Wss1 acts in a Tdp1-independent repair pathway of Top1-mediated DNA damage [25]. In higher eukaryotes, the metalloprotease SPARTAN, which bears similarities with Wss1 [28], has been proposed to be essential for the DPC repair during replication [18, 29, 30, 65]. Recently, another protease, Ddi1, has been found in yeast to be also involved

in the degradation of Top1cc and DPCs in general [66], suggesting a spectrum of proteases required for DPC repair and reflecting the variability of protein-DNA cross-links.

Another possible pathway for making the cleavage site accessible for nucleases could require unfolding or dislodgement of TOP1 from DNA, which is supported by the ability of MUS81 complexes to cleave DNA linked to streptavidin. For example, a helicase or binding proteins may partially displace TOP1, making it more accessible for cleavage. Indeed, we have previously described the ability of the budding yeast Srs2 and Rad54 translocases to directly interact and stimulate Mus81-Mms4 nuclease activity [67, 68]. Similarly, human RecQ5 helicase binds and enhances the enzymatic activity MUS81-EME1 through their physical interaction [69]. In addition, the post-translational modification of TOP1 could lead to a conformational change resulting in the weakening of DNA binding, as has been reported for Rad52 and other proteins [70–72]. Accordingly, the SUMOylation induces TOP2 remodelling and makes the phosphotyrosyl-DNA bond accessible for Tyrosyl-DNA phosphodiesterase 2 (TDP2) hydrolysis [73, 74] and parylation is required for TDP1-dependent repair of TOP1ccs [58].

The ability of MUS81 to cleave a DPC-mimicking substrate in nuclear extracts indicates that MUS81 could possess the same activity *in vivo*, contrary to what was proposed before [75]. Their conclusion was based on the fact that no accumulation of TOP1ccs after the treatment of MUS81-depleted cells with CPT was observed, in contrast to the results observed in TDP1-depleted cells [75]. However, the anti-TOP1 antibodies may not detect proteolytically processed TOP1ccs complexes and that higher number of trapped TOP1 could have been detected in MUS81 TDP1 double mutant. Nevertheless, another explanation for this discrepancy might reflect differences in a cell line, cell-cycle phase, DNA structure or metabolic process. The role of MUS81 in processing DPCs is also supported by induced CPT hypersensitivity of MUS81-KO cells upon depletion of TDP1, indicating that MUS81 and TDP1 play parallel roles in the repair of CPT-induced damage. In agreement, MUS81 also appeared to be crucial for DPC repair in plants, where the *mus81-1* mutant was highly sensitive to CPT [18]. The role of MUS81 and TDP1 in separate pathways is also supported by the observed proliferation defect in unstressed MUS81- and TDP1-deficient cells. These data are in agreement with the detected reduction in plant size of the *tdp1-4 mus81-1* double mutant in *Arabidopsis thaliana* [18]. Based on the available data, we propose a model where TDP1 primarily acts on transcription-associated TOP1ccs and result in the formation of

single-strand breaks (SSBs) (Fig. 6). On the other hand, MUS81 generates DSBs at stalled replication forks in response to CPT or DNA-crosslinking agents [45, 75, 76] as well as reversed forks [77]. Alternatively, direct cleavage of DPCs/TOPcc by MUS81 leads to the generation of SSB that can be converted to DSB by replication run-off [15]. However, the formation of single-strand gaps might also represent a substrate for post-replicative repair and representing a hallmark for improving cancer therapy [78]. Finally, Zhang and colleagues suggested TOP1-induced DSBs formation in non-dividing cells by cleavage of R-loops [79]. Indeed, MUS81 could also preferentially act on unrepaired DPCs at the G2/M phase when it is activated by phosphorylation [80]. However, DSB formation would require cooperation with other nucleases, most likely components of the SMX nuclease complex containing SLX1-SLX4/XPF-ERCC1/MUS81-EME1 [81].

Given the broader spectrum of MUS81 substrates, it may also act on other types of DNA-protein cross-links (DPCs), like those that arise upon exposure to agents such as ionising radiation, UV light, metals and reactive aldehydes, including formaldehyde [82]. This might perhaps explain our observation, that in contrast to TDP1, the sensitivity of MUS81-KO or TDP1/MUS81 double

mutant to CPT is only partially suppressed by TOP1 depletion, most likely reflecting topoisomerase-independent toxicity of CPT [83, 84]. Homologous recombination (HR) and nucleotide excision repair (NER) have also been identified to be required to repair DPCs in bacteria. Although NER excises the entire DPC but cannot act on large DPCs, HR excises DPCs independent of their size [60, 85]. The function of MUS81 in the resolution of recombination intermediates, together with the required proteolytical processing, suggests its more general role in the repair of various DPCs.

However, co-depleted cells can still proliferate, indicating that other repair pathways exist to deal with DPCs. In budding yeast, it has been shown that Mus81-Mms4, Rad1-Rad10 or Mre11 take part in the repair of Top1ccs in addition to the Tdp1 pathway. The *RAD1-TDP1* double mutant showed hypersensitivity to CPT [33], and the *RAD1-TDP1-MUS81* triple mutant presented even higher sensitivity [32]. Moreover, assays with budding yeast indicate that also Rad52 is essential for Top1ccs repair [22, 33], reflecting the importance of homologous recombination. Studies using a suicide Top1 mutant indicate that *RAD52* and *TDP1* are epistatic and that there are other Rad52-dependent pathways in addition to the

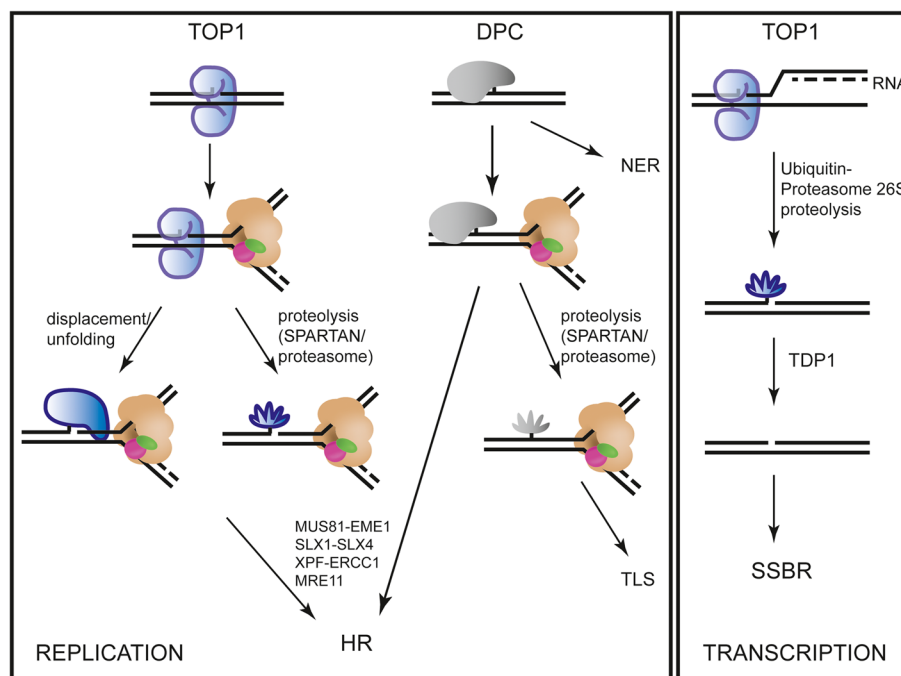


Fig. 6 A possible model for TOP1cc and DPC repair. TOP1ccs (blue) and other DPCs (grey) represent a block for the replication CMG complex (beige). To remove a TOP1cc, it has to be either degraded by the proteasome or proteases (i.e. SPARTAN) or alternatively displaced/unfolded from DNA. Next, the processed TOP1 can be cleaved by a nuclease, such as MUS81-EME1, SLX1-SLX4, XPF-ERCC1 or MRE11, followed by homologous recombination (HR). DPCs that NER does not remove can also undergo proteolysis by a protease or proteasome, followed by translesion synthesis (TLS). Alternatively, DPCs can be removed by the action of the nucleases and repaired by HR. When a TOP1cc blocks transcription, TOP1 is degraded in a ubiquitin/proteasome 26S-dependent manner. TDP1 then removes the remaining TOP1 peptide and the break is repaired by a single-strand break repair pathway (SSBR)

Tdp1 pathway [22]. In addition, an *MRE11* mutant strain appeared to be more sensitive to CPT than the *RAD52* strain, and the sensitivity of this *MRE11* strain is abolished when *TOP1* is disrupted [32]. Indeed, a protein block on DNA was shown to stimulate endonuclease cleavage by the yeast Mre11 complex and could represent a means through which MRE11 plays a role not only in the removal of Spo11 linked to DNA during meiosis [86] but also in the removal of other DPCs. Additionally, it has been shown that TDP2 not only removes TOP2 DPCs but can also process TOP1cc in the absence of TDP1 [87–89].

Conclusions

Our data show the ability of MUS81 complexes to cleave proteolytically processed TOP1ccs and model DPCs as efficiently as various DNA junctions and point to their direct role not only later in the processing of recombination intermediates but also early in cross-link repair. Persistent TOP1ccs are relevant for the success of chemotherapy because the generation of DSBs is believed to underline the anti-cancer properties of CPT derivatives. However, it may as well lead to the formation of single-strand gaps that represent a cancer hallmark considered for improving cancer therapy outcomes and overcoming resistance [78]. In addition, another topoisomerase poison (irinotecan) combined with a proteasome inhibitor showed higher tumour growth inhibition in mice [90]. Proteasome inhibitors have been found to improve the effect of CPT against colorectal cancer [91] or pancreatic cell lines [92]. CPT derivatives are also being studied for clinical use in combination with DNA damage response inhibitors such as PARP1i, ATRi and CHK1i, or immunotherapy [93]. Therefore, these data suggest that targeting MUS81 and other repair pathways dealing with TOP1ccs or other DPCs may represent a new therapeutic and more specific strategy.

Methods

Preparation of unmodified or streptavidin-bound DNA substrates

Synthetic oligonucleotides were purchased from Eurofins Genomics. The sequences and structures are listed in Additional file 7: Table S1 and Additional file 1: Fig. S1, respectively. The fluorescein label at the particular oligonucleotides is indicated by an asterisk. All substrates were prepared according to Marini et al. [94]. Briefly, equimolar amounts of the corresponding oligonucleotides were mixed in hybridising buffer (50 mM Tris, 100 mM NaCl and 10 mM MgCl₂), heated to 75 °C for 3 min and cooled slowly to room temperature for annealing. The substrates were then purified by HPLC using a 1-mL Mono Q column (GE Healthcare Life Sciences) and

a 20-mL gradient in 10 mM Tris buffer containing up to 1 M NaCl. The purity was checked on the native PAGE. The corresponding fractions were then concentrated on a Vivaspin Concentrator 5000 MWCO and washed with buffer W (25 mM Tris and 3 mM MgCl₂). The concentrations were determined using the absorbance at 260 nm and the corresponding molar extinction coefficients. Streptavidin was conjugated to biotin-labelled substrates by incubation for 1 h at room temperature with an equimolar amount of streptavidin.

Preparation of native and trypsinised TOP1 suicide DNA substrates

Synthetic oligonucleotides were purchased from Eurofins Genomics. The oligonucleotide oligo 7 (Additional file 3: Fig. S3B, Additional file 7: Table S1), labelled with fluorescein at the 5' end, contains a preferred TOP1 recognition sequence that allows the cleavage of and covalent binding to TOP1 [95]. After DNA cleavage by TOP1, the last three 3' end nucleotides are released (to yield oligo 7⁻). Oligonucleotides 8, 9 and 12 were first phosphorylated at the 5' end to avoid any possible ligation due to TOP1 activity (Additional file 4: Supplementary methods). A nicked DNA duplex, in which the full-length native TOP1 is bound to the 3' end of the break (Additional file 1: Fig. S1D), was prepared by the hybridisation of oligos 7 (75 pmol), 9 (150 pmol) and 8 (200 pmol) in TOP buffer (5 mM MgCl₂ and 10 mM Tris, pH 7.5) in a total volume of 75 µL. The mixture was heated to 75 °C and cooled down slowly to RT. Then, 10 pmol of this substrate was incubated with 17 pmol of TOP1 in TOP buffer in a total volume of 600 µL for 2 h at 37 °C. The substrate was then maintained at 4 °C and remained stable for approximately 2 weeks.

Trypsinised substrates to which a protease-resistant TOP1-derived peptide remains covalently attached were prepared by digestion with trypsin (Additional file 1: Fig. S1E). Based on the trypsin-cleavage pattern and TOP1 sequence, we estimate that a 7-amino-acid peptide (from Leu721 to Arg727) remains attached to DNA. The trypsinised nicked duplex was prepared from the native TOP1-nicked duplex described above. The native substrate (180 µL) was precipitated with NaCl/ethanol, and 60 µL of activated trypsin (1 µg/µL in 10 mM Tris, pH 7.8) was then added. The mixture was incubated at 37 °C for 45 min. TOP buffer was added to obtain a final reaction volume of 100 µL, and the sample was heated to 75 °C for 5 min. An additional 3 pmol of oligo 9 and 5 pmol of oligo 8 were added, and the sample was allowed to cool down. Aliquots were maintained at -20 °C. The preparation of the 3' flap and Y-form with trypsinised TOP1 bound to the 3' end of the single-stranded part of the substrates (Additional file 1: Fig. S1E) is schematically

explained in Additional file 3: Fig. S3A and in Additional file 4: Supplementary methods.

Expression and purification of TDP1

The TDP1 construct was transformed into BL21 competent cells. The cells were grown in 2 L of 2×TY media containing 50 µg/mL ampicillin to an A_{600} of 0.9 before protein expression was induced with 1 mM of isopropyl-1-thio-β-D-galactopyranoside. The induction proceeded for 2 h at 37 °C, and the cells were then cooled down for 15 min on ice and harvested by centrifugation. The pellets were flash-frozen in liquid nitrogen and stored at −80 °C.

The purification was performed based on the protocol described previously [96]. The pellet was resuspended in 160 mL of binding buffer (0.5 M NaCl, 5 mM imidazole, 20 mM Tris pH 7.9, 1 mM PMSF and 1 mM DTT) and sonicated. The crude lysate was clarified by centrifugation, and the supernatant was filtered through a 45-µm filter and loaded onto a 2-mL nickel column (Ni-NTA Superflow, Qiagen) previously equilibrated with binding buffer. The column was washed with 20 mL of binding buffer and then with 40 mL of binding buffer containing 60 mM imidazole. The protein was eluted with 20 mL of elution buffer (0.5 M NaCl, 150 mM imidazole and 20 mM Tris, pH 7.9). The eluate was collected in 0.5-mL fractions and stored in 50% glycerol at −20 °C.

Purification of TOP1

TOP1 was expressed in the yeast *S. cerevisiae* RS190, which lacks the endogenous TOP1 gene and was purified by column chromatography using a heparin sepharose and phenyl sepharose matrix, as described previously [97].

Purification of MUS81 complexes

The full-length MUS81-EME1 and MUS81-EME2 expression constructs were a kind gift from Stephen West (Cancer Research, UK). The truncated version of MUS81-EME1 used in Additional file 2: Fig. S2A was expressed using MUS81(246-551)-EME1(178-570) expression plasmid, a kind gift of Yunje Cho (Postech, South Korea). Site-directed mutagenesis was used to generate MUS81-nuclease deficient mutant (D338A, D339A) using primers TGCTGCTGCAAAGGGCAGCCAGTCGCTTGC GC and GCGCAAGCGACTGGCTGCCCTTTGCAG CAGCA. The expression was performed as described previously [38], and the purification was performed as published previously [68]. Briefly, the bacterial cells were harvested and resuspended in lysis buffer (50 mM Tris-HCl, pH 7.5, 10% sucrose, 150 mM KCl, 10 mM EDTA, 1 mM DTT, 0.01% Nonidet® P40 (substitute) and protease inhibitors) and sonicated. The lysate was clarified

by centrifugation and loaded sequentially into Q-sepharose and SP-sepharose columns (GE Healthcare). The protein was eluted from the SP column with a 150 to 850 mM KCl gradient in buffer K (20 mM K_2HPO_4 , 10% glycerol, 0.5 mM EDTA, 1 mM DTT and 0.01% Nonidet® P40 (substitute)). The protein-containing fractions were bound to His-Select nickel affinity gel (Sigma-Aldrich) and eluted with increasing concentrations of imidazole (50, 150, 300, 500 mM and 1 M) in buffer K with 150 mM KCl. The fractions with protein were pooled, and their conductivity was adjusted before loading onto a heparin column. The protein complexes were eluted with a gradient from 250 to 900 mM KCl in buffer K, pooled, concentrated and stored in aliquots at −80 °C. The expression and purification of the *S. cerevisiae* Mus81-Mms4 complex were performed as described previously [68]. Briefly, the bacterial cells were resuspended in lysis buffer (50 mM Tris-HCl, pH 7.5, 10% sucrose, 150 mM KCl, 10 mM EDTA, 1 mM DTT, 0.01% Nonidet® P40 (substitute) and protease inhibitors) and sonicated. The crude lysate was clarified by centrifugation. The supernatant was loaded sequentially into Q-sepharose and SP-sepharose columns, and the protein was eluted from the SP column with a 150 to 1000 mM KCl gradient in buffer K. The fractions containing the protein were pooled and bound to a His-Select nickel affinity gel. The complex was eluted with 50, 150 and 300 mM imidazole in buffer K with 150 mM KCl. The fractions containing the complex were pooled, loaded onto a hydroxyapatite column and subsequently eluted with a 0 to 500 mM KH_2PO_4 gradient. Finally, the Mus81-Mms4-containing fractions were pooled, loaded onto a MonoS column and eluted with a 150 to 1000 mM KCl gradient in buffer K. The protein complex was concentrated and stored in aliquots at −80 °C. All final pools were checked on SDS-PAGE (Additional file 8: Fig. S6).

Nuclear extracts

Human breast cancer CAL51 wild-type (WT) and MUS81 knockout (KO) cell lines were cultured in DMEM+10% FBS, supplemented with L-Glutamine and Penicillin–Streptomycin until confluency. Cells were washed twice with cold PBS, scraped from the flask surface and resuspended in PBS. After spinning the cells down at 4°C, 1500 RPM for 3 min, PBS was removed and the cells were resuspended in buffer A (20 mM Tris-HCl pH 7.5, 10 mM NaCl, 3 mM $MgCl_2$, protease inhibitors). After the addition of Nonidet® P40 (substitute) to 0.4%, the cells were incubated for 20 min in ice. Following centrifugation at 4°C and 1500 RPM for 8 min, the supernatant corresponding to the cytosolic fraction was removed. The pellet was resuspended in buffer B (20 mM Tris pH 7.5, 3 mM $MgCl_2$, 410 mM NaCl, 10%

glycerol, 1% Triton-X, protease inhibitors). Sonication was then performed in Bioruptor XL (Diagenode) set to $15 \times [15 \text{ s} + 35 \text{ s rest}]$. After centrifugation at maximal speed, the supernatant, now the nuclear extract, was recovered, aliquoted and stored at -80°C . Protein concentration was measured by Bradford assay.

Nuclease assay

The DNA substrate (3 nM fluorescein-only or streptavidin-linked substrates and 5 nM trypsinised substrates) was incubated at 37°C with the indicated amounts of MUS81-EME1, MUS81-EME2 or Mus81-Mms4 in buffer ME (50 mM Tris pH 7.5, 100 mM KCl, 100 $\mu\text{g}/\text{mL}$ BSA, 1 mM DTT and 5 mM MgCl_2) for 15 min except for the reactions of Mus81-Mms4 with fluorescein-only or streptavidin-linked substrates, which were incubated at 30°C in buffer MM (20 mM Tris pH 7.5, 100 mM KCl, 100 $\mu\text{g}/\text{mL}$ BSA, 0.2 mM DTT, 10 mM MgCl_2 and 5% glycerol). The reaction was stopped with 0.23% SDS and 0.5 mg/mL proteinase K or only SDS in the case of the trypsinised substrates. The samples were then incubated for an additional 3 min at the corresponding temperature, and this step was followed by the addition of loading buffer (for native gels: 10 mM Tris-HCl, 60% glycerol and 60 mM EDTA; for denaturing gels: formamide and bromphenol blue). The reaction products were then resolved by electrophoresis on a native polyacrylamide gel in TBE buffer. The trypsinised substrates were resolved on 6 M urea-denaturing PAGE. In the reaction with the native TOP1 nicked duplex, increasing concentrations of MUS81-EME1 were incubated with 8 nM substrate at 37°C for 15 min. The reaction was stopped with 0.6% SDS and incubated for 4 min; the samples were run on a native PAGE, scanned with a FLA-9000 Starion image scanner (Fujifilm) and analysed with Multi Gauge software (Fujifilm). The scanner was later replaced by Amersham Typhoon RGB (Cytiva). For the assay with nuclear extracts, 20 nM of the streptavidin-linked nicked duplex was incubated with the indicated concentrations of CAL51 WT or MUS81-KO nuclear extracts for 1 h at 37°C . The reaction was stopped by adding SDS and proteinase K, followed by an incubation of 10 min at 37°C . Loading buffer was added, and samples were resolved on a 16% 6 M urea denaturing PAGE. A control sample with purified MUS81-EME1 was also included.

Cleavage assays with TDP1

Increasing amounts of TDP1 were incubated with 8 nM native TOP1 nicked duplex at 30°C for 15 min in buffer T (10 mM Tris pH 8, 100 mM KCl, 1 mM EDTA and 1 mM DTT). The reaction was stopped by adding SDS to

a concentration of 0.6% and incubated for 4 min, and the samples were run on a native PAGE.

Similarly, 5 nM trypsinised substrate was incubated at 30°C with the indicated concentrations of TDP1 in buffer T for 15 min. The reaction was stopped by 0.2% SDS, and the samples were incubated for an additional 3 min. After adding loading buffer (formamide and bromphenol blue), the reaction products were resolved on 6 M urea-denaturing PAGE, and the gels were scanned with a FLA-9000 Starion image scanner (Fujifilm) and analysed with Multi Gauge software (Fujifilm).

Cell culture and drug treatment

CAL51 MUS81-KO stable cell line was generated by the CRISPR-Cas9 system. First, gRNA sequence CAC CGCTGCAGCGGCACCGAACAT was cloned into pSpCas9(BB)-2A-GFP (PX458). Then, CAL51 cells were transiently transfected with the generated plasmid using Lipofectamine 3000 (Thermo Fisher), followed by a selection of GFP-positive single cells using FACS sorter (BD FACS Aria II). The obtained eight clones were later subjected to Western blot, and clone 2 was selected for further use (Additional file 6: Fig. S5A). CAL51 WT and MUS81-KO cell lines were cultured in DMEM + 10% FBS, supplemented with L-Glutamine and Penicillin-Streptomycin. 3×10^5 cells were reverse transfected with 40 nM siRNA pools from Dharmacon either siControl (siCon, #D-001210-01-20), siTDP1 (#M-016112-01-0005) or siTOP1 (OriGene #SR322073) using DharmaFECT 1 reagent (Genetica #T-2001-02) as recommended by the provider. From the transfected-cell suspension, 5×10^3 cells were seeded in each well of a 96-well plate. Parallely, cells were transfected for knockdown assessment by Western blot in a 6-well plate. The cells were allowed to attach and grow for 3–4 days, at the end of which, cell proliferation was assessed using WST-1 (Roche #11644807001) assay as per the manufacturer's protocol.

Western blot analysis

CAL51 WT and MUS81-KO cells were harvested 3–4 days post-transfection with the corresponding siRNA, washed in PBS and lysed in RIPA buffer (Sigma Aldrich # R0278) supplemented with protease and phosphatase inhibitors (Roche; # 000000011836170001 and # 04906837001). Protein concentration was assessed by Bradford assay, and 20–30 μg protein was resolved on a 12% SDS-PAGE. Following antibodies were used to detect TDP1, MUS81 and TOP1: anti-TDP1 (Abcam #ab4166, 1:1000 solution), anti-TOP1 (Abcam #ab109374, 1:10000 solution), anti-MUS81 (Abcam #ab14387, 1:1000 solution) and anti-Actin antibodies (Abcam #ab8226, 1:5000 solution).

Abbreviations

DPC	DNA-protein cross-link
CPT	Camptothecin
DSB	Double-strand break
SSB	Single-strand breaks
NER	Nucleotide excision repair
KO	Knockout
PAGE	Polyacrylamide gel electrophoresis
HPLC	High-performance liquid chromatography
PMSF	Phenylmethylsulfonyl fluoride
DTT	Dithiothreitol
BSA	Bovine serum albumin
EDTA	Ethylenediaminetetraacetic acid
FBS	Fetal bovine serum
PBS	Phosphate-buffered saline
TBE	Tris/Borate/EDTA buffer
SDS	Sodium dodecyl sulphate
GFP	Green fluorescent protein
DMEM	Dulbecco's modified Eagle medium
RIPA	Radioimmunoprecipitation assay buffer
siRNA	Small interfering RNA
oligo	Oligonucleotide

Supplementary Information

The online version contains supplementary material available at <https://doi.org/10.1186/s12915-023-01614-1>.

Additional file 1: Figure S1. Schematics of the DNA substrates used in this study. Each substrate contains one fluorescently labelled oligonucleotide. The 5' end of this fluorescent oligonucleotide is marked. The numbers in italics represent the numbers assigned to the oligonucleotides as indicated in Additional file 7: Table S1. Oligo 7' lacks the last three nucleotides after TOP1 cleavage. Substrates labelled with fluorescein at the 3' position. Standard 3' flap substrate. Substrates modified with biotin to which streptavidin is attached. Nicked duplex with native TOP1 bound to the 3' end of the nick. Substrates that have been treated with trypsin to degrade TOP1 to leave only a tiny peptide bound to the DNA. Substrate modified with biotin to which streptavidin is attached. Free ends are modified with three consecutive thio-bonds.

Additional file 2: Figure S2. Processing of nicked duplexes by MUS81 complexes. Nuclease activity of MUS81-EME1 wild-type or nuclease-dead nicked duplex labelled with CY5 and fluorescein. Products were resolved in native PAGE, and the gel was scanned for both fluorescent labels and images were overlaid. The gel was artificially coloured by the processing software. Nuclease activity of MUS81-EME1 on two nicked duplexes, one with fluorescein at the 3' end of the nick and the other with fluorescein at 5' end of the same oligonucleotide. The bottom strand was labelled with CY5 in both cases. Products were resolved in denaturing PAGE, and the gel was scanned for both fluorescent labels. Oligos of the indicated lengths and labelled with fluorescein were used as marker.

Additional file 3: Figure S3. Preparation of trypsinised substrates. Schematic of the steps required to prepare Y-form and 3' flap trypsinised substrates, as explained in the Methods section. The sequence of oligo 7 shows the TOP1 cleaving site. The last three nucleotides AGA are cleaved off with TOP1 enzyme linked to the shorter oligonucleotide denoted oligo 7'. Three different structures were generated: nicked duplex, Y-form and 3' flap. The denaturing gel of the trypsinised substrates with two major bands: the faster-migrating band corresponds to the unmodified oligonucleotide, indicating a not fully efficient reaction of TOP1 with DNA, and the slower-migrating band corresponds to the oligonucleotide bearing the TOP1 peptide. All of the bands correspond to the fluorescent single-stranded oligonucleotide.

Additional file 4: Supplementary methods. Additional information for the preparation of the trypsinised substrate. Phosphorylation of oligonucleotides; Preparation of 3' flap and Y-form with trypsinised TOP1.

Additional file 5: Figure S4. Quantification of MUS81 nuclease activity on 3' flap unmodified or bearing a peptide. Quantification of MUS81-EME1,

MUS81-EME2 and Mus81-Mms4 nuclease activities on a 3' flap substrate. Comparison of the 3' flap and the 3' flap carrying the TOP1 peptide after trypsin treatment.

Additional file 6: Figure S5. Additional cell-based experiments data. Verification of MUS81 knockout clones by Western blot. Clone 2 was chosen for further experiments. Actin was used as a loading reference. Sensitivity of CAL51 and CAL51 MUS81-KO cells to the indicated concentrations of CPT, with or without TDP1 depletion, measured by WST-1 assay. DMSO was added to the control cells. For each cell line, the results were normalised to the control cells. The means and standard deviations from three independent experiments are shown. The P values were calculated through a multiple unpaired t-test. Individual data values can be found in Additional file 10.

Additional file 7: Table S1. Oligonucleotides constituting the substrates used in this work. A list of sequences of oligonucleotides used for individual synthetic substrates is depicted in Additional file 1: Fig. S1. The end modifications -flu and -biotin are indicated, as well as the thio-bonds. The auxiliary oligonucleotides were used to prepare the trypsinised substrates Y-form and 3' flap but do not constitute the substrates.

Additional file 8: Figure S6. Quality of MUS81 complexes assessed by SDS-PAGE. SDS-PAGE of full-length budding yeast Mus81-Mms4 and human MUS81-EME1 and MUS81-EME2 stained with Coomassie blue and scanned using Typhoon RGB imager. SDS-PAGE of truncated human complex MUS81-EME1 wild-type and nuclease-dead stained with Coomassie® Brilliant Blue R-250 and scanned using Typhoon RGB imager. Protein marker of the indicated molecular weights was included.

Additional file 9. Uncropped images of gels and Western blots. Uncropped images of gels and Western blots shown in this paper.

Additional file 10. Individual data values. Individual data values used for the graphs present in this paper.

Acknowledgements

We thank Marek Sebesta for providing MUS81-EME2, Alexandra Sisakova for Mus81-Mms4, Kristina Slavikova for the truncated form of MUS81-EME1, Pia Jensen for TDP1 and Noriko Hansen for TOP1 proteins.

Authors' contributions

LK designed the experiments. BRK designed the TOP1 substrates. VM prepared all DNA substrates, performed nuclease assays, produced the nuclear extracts and purified MUS81-EME1. FN generated the knockout cell line and, together with PS, performed part of the cell-based experiments. SJ helped with the preparation of TOP1 substrates. LK and VM wrote the manuscript. All authors read and approved the final manuscript.

Funding

This work was supported by the Czech Science Foundation (21-22593X), Preclinical Progression of New Organic Compounds with Targeted Biological Activity (CZ CZ.02.1.01/0.0/0.0/16_025/0007381), Wellcome Trust collaborative grant 206292/E/17/Z and the Aase and Ejnar Danielsen's Foundation.

Availability of data and materials

All data generated or analysed in this study are included in this published article and its supplementary information files. Uncropped gels and blots are provided in Additional file 9. Individual data values for each graph can be found in Additional file 10.

Declarations

Ethics approval and consent to participate

Not applicable.

Consent for publication

Not applicable.

Competing interests

The authors declare that they have no competing interests.

Received: 16 September 2022 Accepted: 4 May 2023
Published online: 16 May 2023

References

- Weickert P, Stinglee J. DNA-protein crosslinks and their resolution. *Annu Rev Biochem.* 2022;91:157–81.
- Hacker L, Dorn A, Puchta H. Repair of DNA-protein crosslinks in plants. *DNA Repair (Amst).* 2020;87:102787.
- Stinglee J, Bellelli R, Boulton SJ. Mechanisms of DNA-protein crosslink repair. *Nat Rev Mol Cell Biol.* 2017;18(9):563–73.
- Enderle J, Dorn A, Puchta H. DNA- and DNA-protein-crosslink repair in plants. *Int J Mol Sci.* 2019;20(17):4304.
- Ide H, Nakano T, Salem AMH, Shoukamy MI. DNA-protein cross-links: formidable challenges to maintaining genome integrity. *DNA Repair (Amst).* 2018;71:190–7.
- Chen SH, Chan NL, Hsieh TS. New mechanistic and functional insights into DNA topoisomerases. *Annu Rev Biochem.* 2013;82:139–70.
- Wang JC. DNA topoisomerases. *Annu Rev Biochem.* 1996;65:635–92.
- Pourquier P, Ueng LM, Kohlhagen G, Mazumder A, Gupta M, Kohn KW, Pommier Y. Effects of uracil incorporation, DNA mismatches, and abasic sites on cleavage and religation activities of mammalian topoisomerase I. *J Biol Chem.* 1997;272(12):7792–6.
- Pourquier P, Pilon AA, Kohlhagen G, Mazumder A, Sharma A, Pommier Y. Trapping of mammalian topoisomerase I and recombinations induced by damaged DNA containing nicks or gaps. Importance of DNA end phosphorylation and camptothecin effects. *J Biol Chem.* 1997;272(42):26441–7.
- Hsiang YH, Hertzberg R, Hecht S, Liu LF. Camptothecin induces protein-linked DNA breaks via mammalian DNA topoisomerase I. *J Biol Chem.* 1985;260(27):14873–8.
- Hsiang YH, Lihou MG, Liu LF. Arrest of replication forks by drug-stabilized topoisomerase I-DNA cleavable complexes as a mechanism of cell killing by camptothecin. *Cancer Res.* 1989;49(18):5077–82.
- Avemann K, Knippers R, Koller T, Sogo JM. Camptothecin, a specific inhibitor of type I DNA topoisomerase, induces DNA breakage at replication forks. *Mol Cell Biol.* 1988;8(8):3026–34.
- Nielsen I, Bentsen IB, Lisby M, Hansen S, Mundbjerg K, Andersen AH, Bjergbaek L. A Flp-nick system to study repair of a single protein-bound nick in vivo. *Nat Methods.* 2009;6(10):753–7.
- Ryan AJ, Squires S, Strutt HL, Evans A, Johnson RT. Different fates of camptothecin-induced replication fork-associated double-strand DNA breaks in mammalian cells. *Carcinogenesis.* 1994;15(5):823–8.
- Strumberg D, Pilon AA, Smith M, Hickey R, Malkas L, Pommier Y. Conversion of topoisomerase I cleavage complexes on the leading strand of ribosomal DNA into 5'-phosphorylated DNA double-strand breaks by replication runoff. *Mol Cell Biol.* 2000;20(11):3977–87.
- Cristini A, Park JH, Capranico G, Legube G, Favre G, Sordet O. DNA-PK triggers histone ubiquitination and signaling in response to DNA double-strand breaks produced during the repair of transcription-blocking topoisomerase I lesions. *Nucleic Acids Res.* 2016;44(3):1161–78.
- Li TK, Liu LF. Tumor cell death induced by topoisomerase-targeting drugs. *Annu Rev Pharmacol Toxicol.* 2001;41:53–77.
- Enderle J, Dorn A, Beying N, Trapp O, Puchta H. The protease WSS1A, the endonuclease MUS81, and the phosphodiesterase TDP1 are involved in independent pathways of DNA-protein crosslink repair in plants. *Plant Cell.* 2019;31(4):775–90.
- Interthal H, Chen HJ, Champoux JJ. Human Tdp1 cleaves a broad spectrum of substrates, including phosphoamide linkages. *J Biol Chem.* 2005;280(43):36518–28.
- Pouliot JJ, Yao KC, Robertson CA, Nash HA. Yeast gene for a Tyr-DNA phosphodiesterase that repairs topoisomerase I complexes. *Science.* 1999;286(5439):552–5.
- Yang SW, Burgin AB, Huizenga BN, Robertson CA, Yao KC, Nash HA. A eukaryotic enzyme that can disjoin dead-end covalent complexes between DNA and type I topoisomerases. *Proc Natl Acad Sci U S A.* 1996;93(21):11534–9.
- Pouliot JJ, Robertson CA, Nash HA. Pathways for repair of topoisomerase I covalent complexes in *Saccharomyces cerevisiae*. *Genes Cells.* 2001;6(8):677–87.
- Liu C, Pouliot JJ, Nash HA. The role of TDP1 from budding yeast in the repair of DNA damage. *DNA Repair (Amst).* 2004;3(6):593–601.
- Vance JR, Wilson TE. Repair of DNA strand breaks by the overlapping functions of lesion-specific and non-lesion-specific DNA 3' phosphatases. *Mol Cell Biol.* 2001;21(21):7191–8.
- Stinglee J, Schwarz MS, Bloemeke N, Wolf PG, Jentsch S. A DNA-dependent protease involved in DNA-protein crosslink repair. *Cell.* 2014;158(2):327–38.
- Nitiss J, Wang JC. DNA topoisomerase-targeting antitumor drugs can be studied in yeast. *Proc Natl Acad Sci U S A.* 1988;85(20):7501–5.
- Pardo B, Moriel-Carretero M, Vicat T, Aguilera A, Pasero P. Homologous recombination and Mus81 promote replication completion in response to replication fork blockage. *EMBO Rep.* 2020;21(7):e49367.
- Stinglee J, Habermann B, Jentsch S. DNA-protein crosslink repair: proteases as DNA repair enzymes. *Trends Biochem Sci.* 2015;40(2):67–71.
- Lopez-Mosqueda J, Maddi K, Prgomet S, Kalayil S, Marinovic-Terzić I, Terzić J, Dikić I. SPRTN is a mammalian DNA-binding metalloprotease that resolves DNA-protein crosslinks. *Elife.* 2016;5:e21491.
- Vaz B, Popovic M, Newman JA, Fielden J, Aitkenhead H, Halder S, Singh AN, Vendrell I, Fischer R, Torrecilla I, et al. Metalloprotease SPRTN/DVC1 orchestrates replication-coupled DNA-protein crosslink repair. *Mol Cell.* 2016;64(4):704–19.
- Maskey RS, Flatten KS, Sieben CJ, Peterson KL, Baker DJ, Nam HJ, Kim MS, Smyrk TC, Kojima Y, Machida Y, et al. Spartan deficiency causes accumulation of Topoisomerase 1 cleavage complexes and tumorigenesis. *Nucleic Acids Res.* 2017;45(8):4564–76.
- Liu C, Pouliot JJ, Nash HA. Repair of topoisomerase I covalent complexes in the absence of the tyrosyl-DNA phosphodiesterase Tdp1. *Proc Natl Acad Sci U S A.* 2002;99(23):14970–5.
- Vance JR, Wilson TE. Yeast Tdp1 and Rad1-Rad10 function as redundant pathways for repairing Top1 replicative damage. *Proc Natl Acad Sci U S A.* 2002;99(21):13669–74.
- Hartsuiker E, Neale MJ, Carr AM. Distinct requirements for the Rad32(Mre11) nuclease and Ctp1(CtIP) in the removal of covalently bound topoisomerase I and II from DNA. *Mol Cell.* 2009;33(1):17–23.
- Zhang YW, Regairaz M, Seiler JA, Agama KK, Doroshov JH, Pommier Y. Poly(ADP-ribose) polymerase and XPF-ERCC1 participate in distinct pathways for the repair of topoisomerase I-induced DNA damage in mammalian cells. *Nucleic Acids Res.* 2011;39(9):3607–20.
- Bartosova Z, Krejci L. Nucleases in homologous recombination as targets for cancer therapy. *FEBS Lett.* 2014;588(15):2446–56.
- Bastin-Shanower SA, Fricke WM, Mullen JR, Brill SJ. The mechanism of Mus81-Mms4 cleavage site selection distinguishes it from the homologous endonuclease Rad1-Rad10. *Mol Cell Biol.* 2003;23(10):3487–96.
- Ciccia A, Constantinou A, West SC. Identification and characterization of the human mus81-eme1 endonuclease. *J Biol Chem.* 2003;278(27):25172–8.
- Pepe A, West SC. Substrate specificity of the MUS81-EME2 structure selective endonuclease. *Nucleic Acids Res.* 2014;42(6):3833–45.
- Agmon N, Yovel M, Harari Y, Liefshitz B, Kupiec M. The role of Holliday junction resolvases in the repair of spontaneous and induced DNA damage. *Nucleic Acids Res.* 2011;39(16):7009–19.
- Kaliraman V, Mullen JR, Fricke WM, Bastin-Shanower SA, Brill SJ. Functional overlap between Sgs1-Top3 and the Mms4-Mus81 endonuclease. *Genes Dev.* 2001;15(20):2730–40.
- Matos J, Blanco MG, Maslen S, Skehel JM, West SC. Regulatory control of the resolution of DNA recombination intermediates during meiosis and mitosis. *Cell.* 2011;147(1):158–72.
- Falquet B, Rass U. Structure-specific endonucleases and the resolution of chromosome underreplication. *Genes (Basel).* 2019;10(3):232.
- Castor D, Nair N, Déclais AC, Lachaud C, Toth R, Macartney TJ, Lilly DM, Arthur JS, Rouse J. Cooperative control of holliday junction resolution and DNA repair by the SLX1 and MUS81-EME1 nucleases. *Mol Cell.* 2013;52(2):221–33.
- Hanada K, Budzowska M, Modesti M, Maas A, Wyman C, Essers J, Kanaar R. The structure-specific endonuclease Mus81-Eme1 promotes conversion of interstrand DNA crosslinks into double-strand breaks. *EMBO J.* 2006;25(20):4921–32.
- Liu LF, Desai SD, Li TK, Mao Y, Sun M, Sim SP. Mechanism of action of camptothecin. *Ann N Y Acad Sci.* 2000;922:1–10.

47. Delgado JL, Hsieh CM, Chan NL, Hiasa H. Topoisomerases as anticancer targets. *Biochem J*. 2018;475(2):373–98.
48. Buzun K, Bielawska A, Bielawski K, Gornowicz A. DNA topoisomerases as molecular targets for anticancer drugs. *J Enzyme Inhib Med Chem*. 2020;35(1):1781–99.
49. Dexheimer TS, Stephen AG, Fivash MJ, Fisher RJ, Pommier Y. The DNA binding and 3'-end preferential activity of human tyrosyl-DNA phosphodiesterase. *Nucleic Acids Res*. 2010;38(7):2444–52.
50. Chang JH, Kim JJ, Choi JM, Lee JH, Cho Y. Crystal structure of the Mus81-Eme1 complex. *Genes Dev*. 2008;22(8):1093–106.
51. Chen XB, Melchionna R, Denis CM, Gaillard PHL, Blasina A, Van de Weyer I, Boddy MN, Russell P, Vialard J, McGowan CH. Human Mus81-associated endonuclease cleaves Holliday junctions in vitro. *Mol Cell*. 2001;8(5):1117–27.
52. Redinbo MR, Stewart L, Kuhn P, Champoux JJ, Hol WG. Crystal structures of human topoisomerase I in covalent and noncovalent complexes with DNA. *Science*. 1998;279(5356):1504–13.
53. Staker BL, Hjerrild K, Feese MD, Behnke CA, Burgin AB, Stewart L. The mechanism of topoisomerase I poisoning by a camptothecin analog. *Proc Natl Acad Sci U S A*. 2002;99(24):15387–92.
54. Svejstrup JQ, Christiansen K, Andersen AH, Lund K, Westergaard O. Minimal DNA duplex requirements for topoisomerase I-mediated cleavage in vitro. *J Biol Chem*. 1990;265(21):12529–35.
55. Fleury F, Ianou A, Kryukov A, Sukhanova A, Kudelina I, Wynne-Jones A, Bronstein IB, Maizieres M, Berjot M, Dodson GG, et al. Raman and CD spectroscopy of recombinant 68-kDa DNA human topoisomerase I and its complex with suicide DNA-substrate. *Biochemistry*. 1998;37(41):14630–42.
56. Debéthune L, Kohlhaagen G, Grandas A, Pommier Y. Processing of nucleopeptides mimicking the topoisomerase I-DNA covalent complex by tyrosyl-DNA phosphodiesterase. *Nucleic Acids Res*. 2002;30(5):1198–204.
57. Davies DR, Interthal H, Champoux JJ, Hol WG. Crystal structure of a transition state mimic for Tdp1 assembled from vanadate, DNA, and a topoisomerase I-derived peptide. *Chem Biol*. 2003;10(2):139–47.
58. Sun Y, Chen J, Huang SN, Su YP, Wang W, Agama K, Saha S, Jenkins LM, Pascal JM, Pommier Y. PARylation prevents the proteasomal degradation of topoisomerase I DNA-protein crosslinks and induces their deubiquitylation. *Nat Commun*. 2021;12(1):5010.
59. Quievryn G, Zhitkovich A. Loss of DNA-protein crosslinks from formaldehyde-exposed cells occurs through spontaneous hydrolysis and an active repair process linked to proteasome function. *Carcinogenesis*. 2000;21(8):1573–80.
60. Baker DJ, Wuenschell G, Xia L, Termini J, Bates SE, Riggs AD, O'Connor TR. Nucleotide excision repair eliminates unique DNA-protein crosslinks from mammalian cells. *J Biol Chem*. 2007;282(31):22592–604.
61. Desai SD, Liu LF, Vazquez-Abad D, D'Arpa P. Ubiquitin-dependent destruction of topoisomerase I is stimulated by the antitumor drug camptothecin. *J Biol Chem*. 1997;272(39):24159–64.
62. Lin CP, Ban Y, Lyu YL, Liu LF. Proteasome-dependent processing of topoisomerase I-DNA adducts into DNA double strand breaks at arrested replication forks. *J Biol Chem*. 2009;284(41):28084–92.
63. Sakasai R, Teraoka H, Tibbetts RS. Proteasome inhibition suppresses DNA-dependent protein kinase activation caused by camptothecin. *DNA Repair (Amst)*. 2010;9(1):76–82.
64. Tomicic MT, Kaina B. Topoisomerase degradation, DSB repair, p53 and IAPs in cancer cell resistance to camptothecin-like topoisomerase I inhibitors. *Biochim Biophys Acta*. 2013;1835(1):11–27.
65. Stingle J, Bellelli R, Alte F, Hewitt G, Sarek G, Maslen SL, Tsutakawa SE, Borg A, Kjær S, Tainer JA, et al. Mechanism and regulation of DNA-protein crosslink repair by the DNA-dependent metalloprotease SPRTN. *Mol Cell*. 2016;64(4):688–703.
66. Serbyn N, Noireterre A, Bagdiul I, Plank M, Michel AH, Loewith R, Kornmann B, Stutz F. The aspartic protease Ddi1 contributes to DNA-protein crosslink repair in yeast. *Mol Cell*. 2020;77(5):1066–1079.e1069.
67. Chavdarova M, Marini V, Sisakova A, Sedlackova H, Vidasova D, Brill SJ, Lisby M, Krejci L. Srs2 promotes Mus81-Mms4-mediated resolution of recombination intermediates. *Nucleic Acids Res*. 2015;43(7):3626–42.
68. Matulova P, Marini V, Burgess RC, Sisakova A, Kwon Y, Rothstein R, Sung P, Krejci L. Cooperativity of Mus81-Mms4 with Rad54 in the resolution of recombination and replication intermediates. *J Biol Chem*. 2009;284(12):7733–45.
69. Di Marco S, Hasanova Z, Kanagaraj R, Chappidi N, Altmannova V, Menon S, Sedlackova H, Langhoff J, Surendranath K, Hühn D, et al. RECQ5 helicase cooperates with MUS81 endonuclease in processing stalled replication forks at common fragile sites during mitosis. *Mol Cell*. 2017;66(5):658–671.e658.
70. Altmannova V, Eckert-Boulet N, Arneric M, Kolesar P, Chaloupkova R, Damborsky J, Sung P, Zhao X, Lisby M, Krejci L. Rad52 SUMOylation affects the efficiency of the DNA repair. *Nucleic Acids Res*. 2010;38(14):4708–21.
71. Sarangi P, Bartosova Z, Altmannova V, Holland C, Chavdarova M, Lee SE, Krejci L, Zhao X. Sumoylation of the Rad1 nuclease promotes DNA repair and regulates its DNA association. *Nucleic Acids Res*. 2014;42(10):6393–404.
72. Vidasova D, Sarangi P, Kolesar P, Vlasaková D, Slezakova Z, Altmannova V, Nikulenkov F, Anrather D, Gith R, Zhao X, et al. Lif1 SUMOylation and its role in non-homologous end-joining. *Nucleic Acids Res*. 2013;41(10):5341–53.
73. Riccio AA, Schellenberg MJ, Williams RS. Molecular mechanisms of topoisomerase 2 DNA-protein crosslink resolution. *Cell Mol Life Sci*. 2020;77(1):81–91.
74. Schellenberg MJ, Lieberman JA, Herrero-Ruiz A, Butler LR, Williams JG, Muñoz-Cabello AM, Mueller GA, London RE, Cortés-Ledesma F, Williams RS. ZAT1 (ZNF451)-mediated resolution of topoisomerase 2 DNA-protein cross-links. *Science*. 2017;357(6358):1412–6.
75. Regairaz M, Zhang YW, Fu H, Agama KK, Tata N, Agrawal S, Aladjem MI, Pommier Y. Mus81-mediated DNA cleavage resolves replication forks stalled by topoisomerase I-DNA complexes. *J Cell Biol*. 2011;195(5):739–49.
76. Miao ZH, Agama K, Sordet O, Povirk L, Kohn KW, Pommier Y. Hereditary ataxia SCAN1 cells are defective for the repair of transcription-dependent topoisomerase I cleavage complexes. *DNA Repair (Amst)*. 2006;5(12):1489–94.
77. Ray Chaudhuri A, Hashimoto Y, Herrador R, Neelsen KJ, Fachinetti D, Bermejo R, Cocito A, Costanzo V, Lopes M. Topoisomerase I poisoning results in PARP-mediated replication fork reversal. *Nat Struct Mol Biol*. 2012;19(4):417–23.
78. Cong K, Cantor SB. Exploiting replication gaps for cancer therapy. *Mol Cell*. 2022;82(13):2363–9.
79. Zhang H, Xiong Y, Su D, Wang C, Srivastava M, Tang M, Feng X, Huang M, Chen Z, Chen J. TDP1-independent pathways in the process and repair of TOP1-induced DNA damage. *Nat Commun*. 2022;13(1):4240.
80. Palma A, Pugliese GM, Murfunì I, Marabitti V, Malacaria E, Rinalducci S, Minoprio A, Sanchez M, Mazzei F, Zolla L, et al. Phosphorylation by CK2 regulates MUS81/EME1 in mitosis and after replication stress. *Nucleic Acids Res*. 2018;46(10):5109–24.
81. Wyatt HD, Laister RC, Martin SR, Arrowsmith CH, West SC. The SMX DNA repair tri-nuclease. *Mol Cell*. 2017;65(5):848–860.e811.
82. Barker S, Weinfeld M, Murray D. DNA-protein crosslinks: their induction, repair, and biological consequences. *Mutat Res*. 2005;589(2):111–35.
83. Li F, Jiang T, Li Q, Ling X. Camptothecin (CPT) and its derivatives are known to target topoisomerase I (Top1) as their mechanism of action: did we miss something in CPT analogue molecular targets for treating human disease such as cancer? *Am J Cancer Res*. 2017;7(12):2350–94.
84. Mabb AM, Simon JM, King IF, Lee HM, An LK, Philpot BD, Zylka MJ. Topoisomerase 1 regulates gene expression in neurons through cleavage complex-dependent and -independent mechanisms. *PLoS One*. 2016;11(5):e0156439.
85. Nakano T, Morishita S, Katafuchi A, Matsubara M, Horikawa Y, Terato H, Salem AM, Izumi S, Pack SP, Makino K, et al. Nucleotide excision repair and homologous recombination systems commit differentially to the repair of DNA-protein crosslinks. *Mol Cell*. 2007;28(1):147–58.
86. Cannavo E, Cejka P. Sae2 promotes dsDNA endonuclease activity within Mre11-Rad50-Xrs2 to resect DNA breaks. *Nature*. 2014;514(7520):122–5.
87. Cortes Ledesma F, El Khamisy SF, Zuma MC, Osborn K, Caldecott KW. A human 5'-tyrosyl DNA phosphodiesterase that repairs topoisomerase-mediated DNA damage. *Nature*. 2009;461(7264):674–8.
88. Zeng Z, Sharma A, Ju L, Murai J, Umans L, Vermeire L, Pommier Y, Takeda S, Huylebroeck D, Caldecott KW, et al. TDP2 promotes repair of topoisomerase I-mediated DNA damage in the absence of TDP1. *Nucleic Acids Res*. 2012;40(17):8371–80.
89. Tsuda M, Kitamasu K, Kumagai C, Sugiyama K, Nakano T, Ide H. Tyrosyl-DNA phosphodiesterase 2 (TDP2) repairs topoisomerase 1 DNA-protein

- crosslinks and 3'-blocking lesions in the absence of tyrosyl-DNA phosphodiesterase 1 (TDP1). *DNA Repair (Amst)*. 2020;91–92:102849.
90. Lenz HJ. Clinical update: proteasome inhibitors in solid tumors. *Cancer Treat Rev*. 2003;29(Suppl 1):41–8.
 91. Cusack JC, Liu R, Houston M, Abendroth K, Elliott PJ, Adams J, Baldwin AS. Enhanced chemosensitivity to CPT-11 with proteasome inhibitor PS-341: implications for systemic nuclear factor-kappaB inhibition. *Cancer Res*. 2001;61(9):3535–40.
 92. Naumann K, Schmich K, Jaeger C, Kratz F, Merfort I. Noxa/Mcl-1 balance influences the effect of the proteasome inhibitor MG-132 in combination with anticancer agents in pancreatic cancer cell lines. *Anticancer Drugs*. 2012;23(6):614–26.
 93. Talukdar A, Kundu B, Sarkar D, Goon S, Mondal MA. Topoisomerase I inhibitors: challenges, progress and the road ahead. *Eur J Med Chem*. 2022;236:114304.
 94. Marini V, Krejci L. Unwinding of synthetic replication and recombination substrates by Srs2. *DNA Repair (Amst)*. 2012;11(10):789–98.
 95. Andersen AH, Christiansen K, Westergaard O. Uncoupling of topoisomerase-mediated DNA cleavage and religation. *Methods Mol Biol*. 2001;95:101–17.
 96. Interthal H, Pouliot JJ, Champoux JJ. The tyrosyl-DNA phosphodiesterase Tdp1 is a member of the phospholipase D superfamily. *Proc Natl Acad Sci U S A*. 2001;98(21):12009–14.
 97. Knudsen BR, Straub T, Boege F. Separation and functional analysis of eukaryotic DNA topoisomerases by chromatography and electrophoresis. *J Chromatogr B Biomed Appl*. 1996;684(1–2):307–21.

Publisher's Note

Springer Nature remains neutral with regard to jurisdictional claims in published maps and institutional affiliations.

Ready to submit your research? Choose BMC and benefit from:

- fast, convenient online submission
- thorough peer review by experienced researchers in your field
- rapid publication on acceptance
- support for research data, including large and complex data types
- gold Open Access which fosters wider collaboration and increased citations
- maximum visibility for your research: over 100M website views per year

At BMC, research is always in progress.

Learn more biomedcentral.com/submissions

